An Efficient and Highly Accurate Technique for Periodic Planar Scanner Calibration with the Antenna Under Test in Situ

Scott Pierce
MI Technologies
1125 Satellite Boulevard, Suite 100
Suwanee, Georgia 30024
spierce@mi-technologies.com

Marion Baggett
MI Technologies
1125 Satellite Boulevard, Suite 100
Suwanee, Georgia 30024
mbaggett@mi-technologies.com

ABSTRACT

This paper describes the development, testing and evaluation of a new, automated system for calibration and AUT alignment of a planar near-field scanner that allows the calibration system to remain in place during AUT measurement and which can be used to support AUT alignment to the scan plane. During scanner calibration, probe aperture position measurements are made using a tracking laser interferometer, a fixture that positions the interferometer retro reflector at a precise location relative to the probe aperture and a probe roll axis that maintains the proper orientation between the retro reflector and the interferometer as the probe position is moved. Aperture scan path information is used to construct a best-fit scan plane and to define a Cartesian, scanner-based coordinate system. Scan path data is then used to build a probe position error map for each of the three Cartesian coordinates as a function of the nominal position in the scan plane. These error maps can be used to implement software-based corrections (K-corrections) or they may be used for active Z-axis correction during measurements. By using a set of tooling points on the antenna mount, an AUT coordinate system is measured with the interferometer. The system then directs an operator through a set of AUT adjustments that align the AUT with the planar near-field scanner to a desired accuracy. This paper describes the implementation and testing of the system on an actual planar scanner and AUT test environment, showing the improvement in effective scanner planarity.

Keywords: Planar, Near-field, Error Correction, Scanner, Interferometer

1.0 Introduction

Planar near-field scanning has become a standard method for antenna testing. This method is particularly important in testing high frequency, planar phased-array antennas. At very high frequencies the scan-plane accuracy needed for planar near-field testing begins to exceed the accuracy that can be achieved strictly through physical alignment and control of machining tolerances. Thus, some secondary correction mechanism is needed to improve scan plane planarity and position accuracy. This secondary correction can take the form of a software correction or it may be achieved through active correction of the position of the RF probe aperture during testing. In either case, error correction requires a set of maps of errors in the probe aperture position as a function of probe position and orientation.

In this work, we describe a method for the construction of a set of planar scanner error maps using a calibration system that integrates a tracking laser interferometer with an MI-Technologies microwave measurement and analysis system (Figure 1). The geometry of this calibration system is designed so that error maps can be constructed without moving the antenna under test from its position in front of the scan plane. Maps are constructed by making direct measurements of the spatial position of the RF probe aperture. We demonstrate the construction of X-axis, Y-axis and Z-axis error maps for a planar scanner with a 88 cm. x 88 cm. scan plane. We then demonstrate the use of the Z-axis error map to perform a physical correction of the scan plane geometry and compare the topography of uncorrected and corrected scan planes. We also demonstrate the use of the system to align a test antenna to the corrected scan plane.

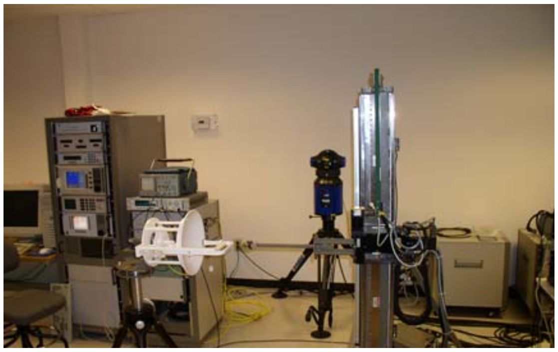

Figure 1: The test apparatus

2.0 System Architecture

Figure 2 shows a schematic representation of the measurement system. The major components of the system are the MI-6900 planar scanner, the MI-2097 Microwave Measurement System, the MI-3001 Data Acquisition and Analysis Workstation and the coordinate metrology system which utilizes a FARO Tracker tracking laser interferometer.

2.1 The Planar Scanner

In this work we use an MI Technologies 6900-Series planar scanner with scan plane dimensions of 88 cm. in the X (horizontal) axis and 88 cm. in the Y (vertical)

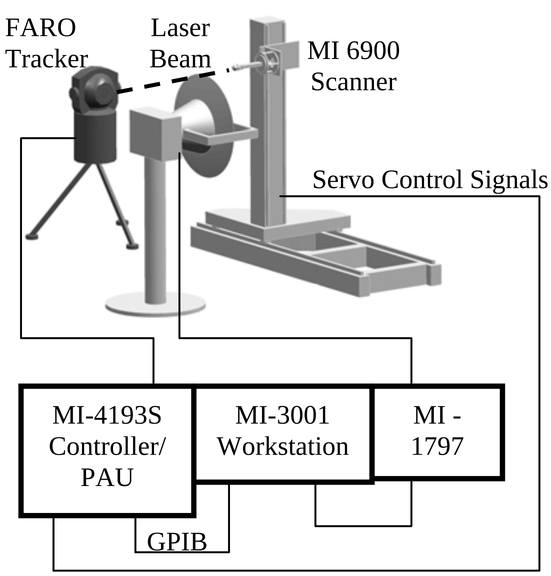

Figure 2: Schematic Diagram of the Measurement System

axis. The planar scanner uses linear servomotor drives and optical linear encoders in the X and Y-axes. The polarization (χ) axis is a rotary, worm-drive rotary stage driven by a DC-servomotor and an optical rotary encoder. The Z-axis (which is used for error correction) is a relatively inexpensive, commercially available positioning slide. It utilizes a DC-servomotor with an optical, rotary encoder driving a linear ball-screw slide.

2.2 The Coordinate Metrology System

In order to measure the spatial position of the probe aperture, we utilize a FARO Tracker tracking laser interferometer, a FARO spherically-mounted retro reflector target (SMR) and a fixture that facilitates accurate positioning of the SMR relative to the aperture of
the probe (Figure 3). The SMR consists of a corner mirror mounted at the center of a steel sphere. By comparing the relative positions of the outgoing and reflected laser beams the Tracker can be made to follow the position of the SMR as it moves through space. The SMR mounting fixture consists of a pair of precision-machined components that attach to the end of the RF probe and hold the SMR using a magnetic mount. The relative position between the SMR and the probe aperture is measurable and highly repeatable, thus if the position of the SMR is known the position of the probe aperture is known to nearly the same accuracy. The advantage of this approach is that we are very nearly making a direct measurement of the position of the probe aperture. This is in contrast to less direct measurement approaches that measure the position of intermediate points on the scanner carriages. These less direct measurement approaches can fail to detect motion of the probe aperture due to carriage rotations.

The absolute position accuracy of the FARO Tracker is a function of distance from the Tracker laser head and the angles of rotation of the Tracker rotary axes. In this experiment the 2σ accuracy of the Tracker varies across the scan plane from 11 μm. in the area nearest to the Tracker to 27 μm. in the area farthest from the Tracker.

In order for the Tracker to measure the position of the SMR, the aperture of the SMR must point at the laser head of the Tracker to within an angle of +/- 20°. This means that the planar scanner control algorithm must rotate the χ axis of the scanner as the SMR is moved through the scan plane. Implementation of this coordinated motion is discussed in further detail in Section 2.3.

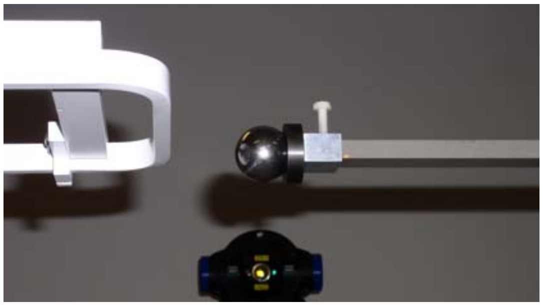

Figure 3: SMR positioned in the mounting fixture.

2.3 The Microwave Measurement System

The MI-2097 Automated Microwave Measurement System consists of the MI-1797 Receiver, the MI-3100 Signal Source and the MI-4193S Position Controller. The MI-4193S is actively involved in the scan plane error mapping process as follows:

- The MI-4193S provides the control of motion for the X, Y and Z axes of the scanner, along with the χ-axis.
- The MI-4193S can implement an error correction map through the use of its coordinated motion feature [1]. A similar map has been used for three-axis probe correction in a large spherical near-field scanning system [2]. This error map can be applied real time to the Z as either the Y or X-axis is scanned or stepped.
- The error map is a simple text file in X, Y and δZ loaded into the MI-4193S. Once the error map is loaded, the MI-4193S can be commanded to use the raw Z-axis or a corrected Z axis based on X and Y positions.

2.4 The Data Acquisition and Analysis System

The MI-3001 Data Acquisition and Analysis Workstation and software provide the computer control of scanner error map data collection and verification operations. The un-corrected scan plane data is collected as a raster scan in X and Y, where the X and Y positions are obtained through a sequence of discrete steps. Through the entire grid, the Z-axis is held at a fixed position. As the X and Y-axes are stepped to a new position in the grid, the polarization axis is moved to an angle that best points the SMR toward the Tracker at that particular location. In this way, the SMR is always pointed at the tracker, preventing loss of tracking during the collection of the grid. At each point, when the scanner axes have been positioned, the software generates a trigger that is sent to the Tracker to trigger a measurement of the position of the SMR.

The entire measurement process is controlled by a Visual Basic script that uses built-in low-level instrument controls for the MI-4193S. Scan plane correction verification is performed by the same script with the corrected Z-axis used instead of the raw Z-axis.

3.0 Error Mapping

The goal of planar scanner error mapping is to map errors in the Cartesian coordinates of the RF probe aperture position as a function of the desired aperture position. Thus, we would like to find:

$$\Delta x\left(x_T, y_T, z_T, \chi_T\right)$$
$$\Delta y\left(x_T, y_T, z_T, \chi_T\right)$$
$$\Delta z^p(x^p, y^p) = z_M^p - z_T^p$$

where:

$\Delta x, \Delta y, \Delta z$ = deviations from the target Cartesian coordinates
x_T, y_T, z_T = target Cartesian coordinates

Figure 4 is a flow chart of the scanner calibration and antenna alignment process. For the work described in this paper, the 88 cm. x 88 cm. scan plane was sampled using a square grid of points that were spaced 2 cm. apart. The choice of sampling grid size was based upon an earlier measurement of the uncorrected scan plane. This measurement showed that the scanner exhibits a roughly periodic error in X that has a period of ~10 cm. and an amplitude of ~120 μm. (Figure 5. Note that the planar scanner was purposely placed in an imperfectly-aligned state for the purposes of this experiment.) A 2 cm. sampling grid is fine enough to ensure that this periodic error is measured.

As shown in Figure 4, error mapping and antenna alignment begins with calibration of the Tracker and mounting of the SMR on the RF probe. Once this procedure is completed, error mapping proceeds as follows:

1. "Home" the scanner. Using the Tracker, measure the spatial position of the SMR. This point will be used as the origin of the Cartesian,

"scanner coordinate system." This is the system in which all error terms will be defined.

2. Measure the nominal Y=0 line in order to define the X-axis of the scanner coordinate system.
3. Measure a grid of points across the scan plane:
    a. Move the probe to one corner of the scan plane.
    b. Measure the spatial position of the SMR for the first grid point.
    c. Iteratively step through the grid, measuring the position of the SMR at

    each grid point. As the probe moves through the scan plane the χ-axis is rotated so that the SMR faces the Tracker.
4. Using the grid data, find the best-fit scan plane using a least-mean squares algorithm. The normal vector to this scan plane defines the direction of the Z-axis of the scanner coordinate system.
5. Map x and y errors as a function of χ:
    a. Step the χ-axis through the range of angles needed to keep the SMR pointed at the laser during scan plane mapping.
    b. At each χ step, measure the position of the Tracker target. Use these measurements to calculate ΔX(χ), ΔY(χ), ΔZ(χ).
6. For each grid point, calculate the components of the x, y and z errors that are caused only by translation of the probe across the scan plane. *These are the terms that are used to generate the x,y and z error maps.* For a given grid point *p* these terms are:

$$\Delta x^p(x_T, y_T) = x_M^p - x_T^p - \Delta x^p(\chi^p)$$
$$\Delta y^p(x_T, y_T) = y_M^p - y_T^p - \Delta y^p(\chi^p)$$
$$\Delta z^p(x^p, y^p) = z_M^p - z_T^p - \Delta z^P(\chi^P)$$

where:

x_M^p, y_M^p, z_M^p = measured coordinates of point *p*

x_T^p, y_T^p, z_T^p = target coordinates of point *p*

$\Delta x^p(\chi^p), \Delta y^p(\chi^p), \Delta z^P(\chi^P)$ = position errors caused by rotating the polarization positioner to the angle χ needed to keep the laser target pointed at the laser when the probe is at point *p*

At this point, the spatial orientation of the scan plane has been defined and the error maps have been constructed.

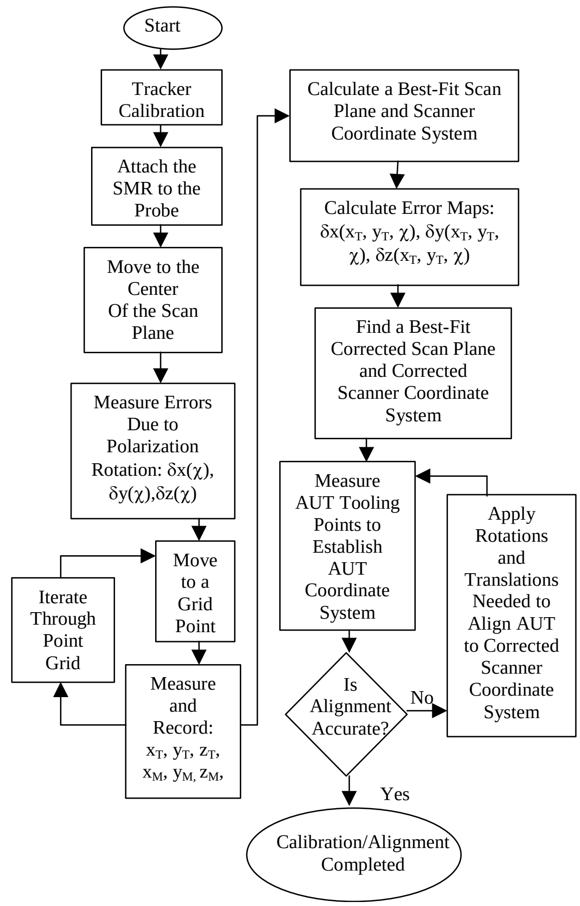

Figure 4: Flow chart of the calibration and alignment process

In this work, the Z-axis error map is utilized to implement active error correction using a linear stage. The effect of this active correction was measured by re-measuring the point grid with the correction enabled. The best-fit plane to this corrected data was then calculated and used as the basis of a corrected scanner coordinate system. AUT alignment was then performed relative to this corrected system.

In order to align the AUT, tooling points that defined an AUT coordinate system were measured using the Tracker. The position of the tooling points relative to the antenna geometry were known from previous Tracker measurements. Once the AUT coordinate system was found, the values of the two rotations about the AUT system X and Y axes that would make the AUT Z-axis parallel with the scanner Z axis were reported by the Tracker software. These two rotations were applied to the AUT and the tooling points were re-measured. This process of measurement and adjustment was iterated until the Z axes of the two coordinate systems were within the required precision. In order to make the Z-axes of the two coordinate systems collinear, the relative positions of the scanner system origin and the AUT system origin were calculated and these values were entered as offsets in the MI-4193S controller. This had the effect of shifting the scanner system into alignment with the AUT system without moving the AUT.

4.0 Results

Figure 5 shows the topography of the scan plane before the implementation of active Z-axis correction. The plane has a periodic error across the X-axis that has a period of ~10 cm. and an amplitude of ~120 μm. In addition to this periodic error the nominally planar surface has some curvature about an axis that runs diagonally across the plane. This curvature is caused by a slight parallelism error between the front and rear X-axis rails. The absolute Z-axis error of the uncorrected scan plane is +170/-93 μm. and the RMS error is 40 μm.

Figure 6 shows the topography of the scan plane after the implementation of active Z-axis correction. Both the periodic error and the overall curvature error have been reduced to levels that are near the limits of the Tracker measurement resolution. The absolute Z-axis error of the corrected scan plane is +35/-37 μm. and the RMS planarity is 10 μm.

5.0 Summary

In this paper we have described a planar scanner error mapping and calibration system that is based on the integration of an MI-2097 Automated Microwave Measurement System with a FARO Tracker tracking laser interferometer. We have shown that this integrated system can be used to make direct measurements of the position of the aperture of an RF probe as it is moved through the scan plane. We have used these measurements to construct error maps of the aperture position.

In order to utilize the map of planarity errors, we implemented active Z-axis correction using a relatively inexpensive linear slide and the coordinated-motion capability of the MI-4193S motion controller. Using this error correction scheme we were able to improve the RMS planarity of the scan plane by a factor of four.

An advantage of our approach is that error mapping can be performed with the AUT in place and the Tracker can then be used to align the AUT. In this paper we demonstrated the use of the measurement system to establish a Cartesian coordinate system based on the corrected scan plane. We then used the Tracker to align an AUT to this corrected scanner coordinate system.

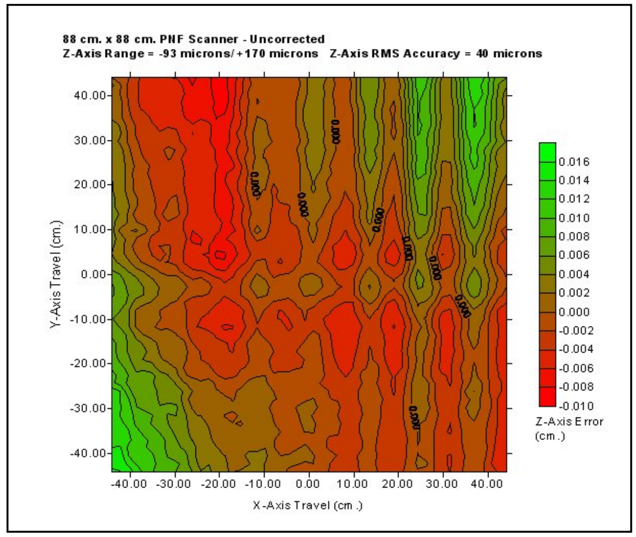

Figure 5: Topography of the uncorrected scan plane

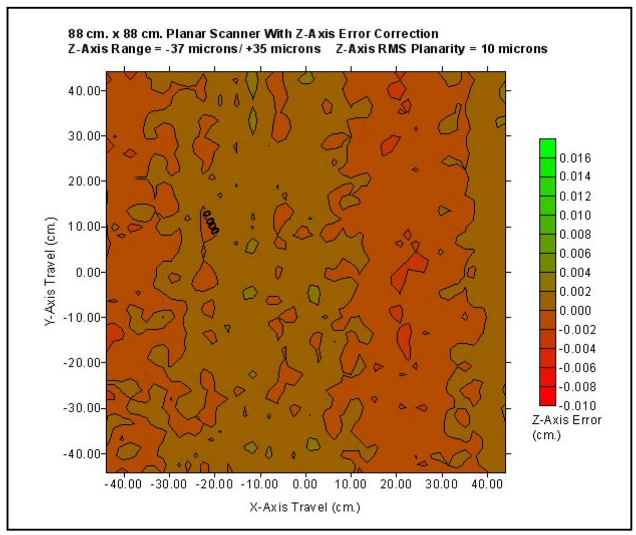

Figure 6: Topography of the corrected scan plane

6.0 REFERENCES

[1] "Applications for Coordinated Motion in Radome Testing ", McBride, et. al., AMTA Symposium 2002, pg 471-476.

[2] "Implementation of a Geometric-Error Correction System for Extremely High Probe Position Accuracy in Spherical Near-Field Scanning", Pierce, R.S. and Langston, J., AMTA Symposium 2004 (Accepted for Publication).

7.0 ACKNOWLEDGMENTS

The authors wish to recognize Dean Darsey, Becky Kaffezakis, Jim Langston, Scott McBride and Don Weiss, all of MI Technologies, for their assistance in the development and operation of this procedure.